Role of Benzyl Alcohol in the Unfolding and Aggregation of Interferon α-2a

REGINA L. BIS, SURINDER M. SINGH, JAVIER CABELLO-VILLEGAS, KRISHNA M. G. MALLELA

Department of Pharmaceutical Sciences & Center for Pharmaceutical Biotechnology, Skaggs School of Pharmacy and Pharmaceutical Sciences, University of Colorado Anschutz Medical Campus, Aurora Colorado 80045

Received 14 April 2014; revised 18 June 2014; accepted 8 July 2014

Published online in Wiley Online Library (wileyonlinelibrary.com). DOI 10.1002/jps.24105

ABSTRACT: Benzyl alcohol (BA) is the most widely used antimicrobial preservative in multidose protein formulations, and has been shown to cause protein aggregation. Our previous work on a model protein cytochrome *c* demonstrated that this phenomenon occurs via partial unfolding. Here, we examine the validity of these results by investigating the effect of BA on a pharmaceutically relevant protein, interferon α-2a (IFNA2). IFNA2 therapeutic formulations available on the pharmaceutical market contain BA as a preservative. Isothermal aggregation kinetics and temperature scanning demonstrated that BA induced IFNA2 aggregation in a concentration-dependent manner. With increasing concentration of BA, the apparent aggregation temperature of IFNA2 linearly decreased. Denaturant melts measured using protein intrinsic fluorescence and that of the 1-anilinonaphthalene-8-sulfonic acid dye indicated that IFNA2 stability decreased with increasing BA concentration, populating a partially unfolded intermediate. Changes in nuclear magnetic resonance chemical shifts and hydrogen exchange rates identified the structural nature of this intermediate, which correlated with an aggregation "hot-spot" predicted by computational methods. These results indicate that BA induces IFNA2 aggregation by partial unfolding rather than global unfolding of the entire protein, and is consistent with our earlier conclusions from model protein studies.

Keywords: protein aggregation; protein folding; protein formulation; excipients; stability; benzyl alcohol; interferon α-2a; NMR

INTRODUCTION

Protein-based pharmaceuticals comprise nearly half of all parenteral products available worldwide.[1,2] One third of these products are available as multidose formulations,[3] which are advantageous for patient compliance as well as economics. In addition to a shelf-life stability requirement of 18–24 months,[4] multidose formulations also necessitate the inclusion of antimicrobial preservatives (APs)[4,5] to combat the growth of bacteria and other microbes during repeated contact between the solution and syringe needle.

In recent years, the study of APs in protein pharmaceutics has become increasingly important because of the fact that these compounds have been shown to cause protein aggregation. One of the first reports demonstrated that the addition of various aromatic and aliphatic alcohols caused aggregation of human growth hormone.[6] In recent studies, APs have been shown to induce the aggregation of numerous protein systems, including interleukin-1 receptor antagonist,[7,8] interferon-γ,[9] and an antibody.[10] Such protein aggregates in formulations can affect the amount and efficacy of the delivered drug as well as promote undesirable immunologic responses in patients.[11–17] Therefore, an understanding of the molecular mechanisms underlying AP-induced protein aggregation and the development of strategies to minimize such aggregation are critical in developing stable multidose drugs.

Previously published work from our laboratory on the model protein cytochrome *c* (Cyt c) demonstrated that local unfolding of the protein, rather than the global unfolding, leads to protein aggregation.[18–20] This local unfolding identified an aggregation "hot-spot" that could be modified to increase protein stability and decrease aggregation. It is important to test these principles learned from model protein studies on a pharmaceutically relevant protein to determine whether these conclusions are general to AP-induced aggregation of proteins. For this purpose, we chose to study interferon α-2a (IFNA2) (Fig. 1). IFNA2 has been shown in the literature to aggregate under formulation conditions.[21–24] Benzyl alcohol (BA) has been used as a preservative in IFNA2 formulations. Whether BA causes IFNA2 aggregation has not been explored. We show that IFNA2 is susceptible to increased aggregation in the presence of BA, and that the aggregation mechanism proceeds through a partially unfolded intermediate. Structural nature of this intermediate has been obtained using 2D nuclear magnetic resonance (NMR), which gives information at the resolution of individual amino acids. Using such high-resolution structural techniques is relatively rare in characterizing pharmaceutical proteins.

MATERIALS AND METHODS

Materials

Synthetic cDNA corresponding to IFNA2 was obtained from Operon (Huntsville, Alabama), and was cloned into the pET-SUMO expression vector[25,26] (a generous gift from Christopher Lima, Sloan-Kettering Institute). Protein was expressed

Abbreviations used: ANS, 1-anilinonaphthalene-8-sulfonic acid; AP, antimicrobial preservative; BA, benzyl alcohol; C_m, midpoint denaturant concentration in protein denaturant melt; Cyt *c*, cytochrome *c*; ΔG, Gibbs free energy of protein unfolding; GdmCl, guanidinium chloride; HSQC, heteronuclear single quantum coherence; HX, hydrogen exchange; IFNA2, interferon α-2a; *m*-value, slope of the linear variation of ΔG with denaturant concentration; NMR, nuclear magnetic resonance; T_m^{Agg}, midpoint aggregation temperature; HSA, human serum albumin.

Correspondence to: Krishna M. G. Mallela (Telephone: +303-724-3576; Fax: +303-724-7266; E-mail: krishna.mallela@ucdenver.edu)

Journal of Pharmaceutical Sciences

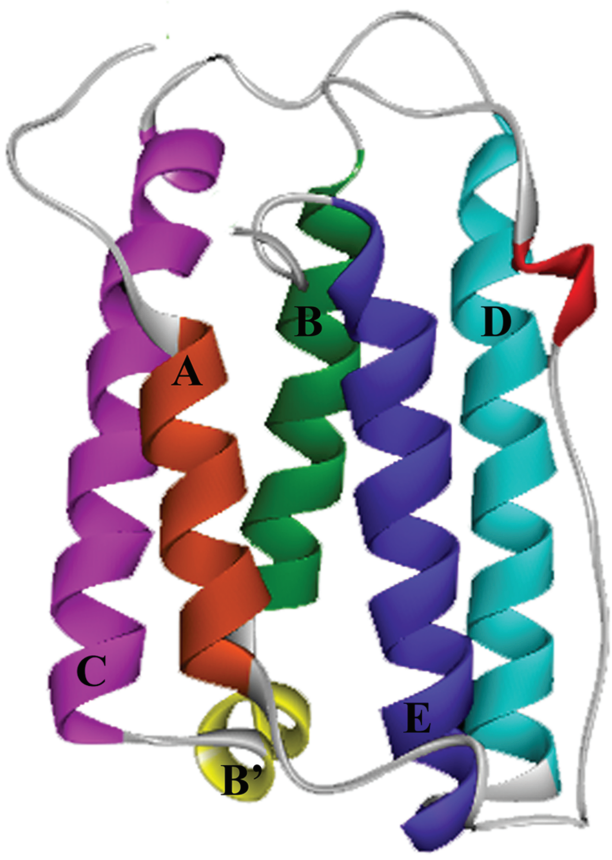

Figure 1. Molecular structure of interferon α-2a (IFNA2) (PDB ID: 1ITF). The protein is α-helical in nature with helices organized according to color: helix A, residues 11–21 (orange); helix B, residues 52–68 (green); helix B′, residues 70–75 (yellow); helix C, residues 78–100 (purple); helix D, residues 110–132 (cyan); helix E, residues 137–157 (blue). Residues 22–51 comprise the AB-loop, and residues 40–43 form a 3_{10} helix (red).

in *Escherichia coli* BL21(DE3) cells, and the soluble protein was purified using a Nickel Sepharose 6 Fast Flow column (GE Healthcare Life Sciences, Pittsburgh, Pennsylvania). The SUMO tag was cleaved using the Ulp1 protease, leaving no additional amino acids. The final protein sequence was identical to that of the pharmaceutical protein, which was confirmed by mass spectrometry, circular dichroism, and NMR. Details of IFNA2 expression, purification, and characterization have been described in our earlier publication.[27]

Size-Exclusion Chromatography

To monitor the effects of BA on protein aggregation, IFNA2 in formulation buffer (10 μM in 0.01 M ammonium acetate, 0.12 M sodium chloride, pH 5) was incubated at 50°C and samples were taken at desired intervals. Samples were centrifuged prior to injection on the HPLC column, and only soluble monomer was detected. Monomer concentration was estimated by injecting 70 μL onto a TSKgel 5 μM G3000SWxl column (Tosoh Bioscience LLC, San Francisco, California) on an Agilent 1100 HPLC (Santa Clara, California). The mobile phase used was 0.01 M ammonium acetate, 0.12 M sodium chloride, pH 5, at a flow rate of 1 mL min^{-1}. Absorbance at 280 nm was used to determine the monomer content.

Isothermal Incubation Experiments

Interferon α-2a (10 μM) in formulation buffer was incubated at the desired temperature, and the changes in optical density at 350 nm were measured as a function of the incubation time.[28] Buffer and protein do not absorb at this wavelength. The aggregation kinetics was monitored until the signal reached a plateau. At longer incubation times, the aggregates started to settle down to the bottom of the cuvette, resulting in decreased optical density. At that point, the experiment was stopped.

Thermal Scanning Method

The midpoint aggregation temperature (T_m^{Agg}) of the protein was measured on an UV-Visible spectrophotometer (Agilent Technologies, Santa Clara, California). The temperature was increased at a rate of 1°C/step followed by 90 s equilibration, and changes in the optical density at 450 nm were monitored.[29] $T_m{}^{Agg}$ was determined as the temperature at which half the maximum optical density was reached. For these experiments, 10 μm IFNA2 in formulation buffer was used with varying BA concentration.

Denaturant Melts

Guanidinium chloride (GdmCl) was used as the denaturant. Protein solutions at varying GdmCl concentrations were prepared and equilibrated for 1 h at room temperature before measuring changes in fluorescence signals as a function of the denaturant concentration. Concentration of the denaturant was determined using refractive index measurements.[30] For measuring changes in the 280 nm (aromatic) fluorescence, 3 μM IFNA2 in formulation buffer was used with varying concentrations of BA. Fluorescence spectra were obtained using a Quantamaster spectrofluorometer (Photon Technology International, Birmingham, New Jersey) with 4 nm slits. The Gibbs free energy of protein unfolding (ΔG) values were determined by fitting the changes in optical signals at different denaturant concentrations to a two-state unfolding model.[31,32] The m-value, which is the slope of linear variation of ΔG with denaturant concentration, was obtained by fitting the data to Santero-Bolen two-state equation.[31,32]

ANS Fluorescence

1-Anilinonaphthalene-8-sulfonic acid (ANS) (Sigma, St. Louis, Missouri) at a concentration of 100 μM was used to monitor partial unfolding of IFNA2. The same experimental setup described above for the denaturant melts was employed for ANS fluorescence experiments. Fluorescence intensity was measured using a Quantamaster spectrofluorometer. Excitation and emission wavelengths used were 360 and 480 nm, respectively, and slit widths were 4 nm. Samples were corrected for ANS and BA fluorescence in the absence of protein. All samples were normalized using a rhodamine cuvette (Starna Cells, Atascadero, California).

Nuclear Magnetic Resonance

BA Titration

2D ^{15}N-^{1}H heteronuclear single quantum coherence (HSQC) experiments were run to monitor changes in IFNA2 amide cross peaks as a function of BA concentration using a Varian Inova 600 MHz NMR instrument equipped with a cryoprobe (Palo Alto, California). IFNA2 was singly labeled with ^{15}N using M9

minimal media and expressed using cold induction for 16 h. For these NMR experiments, 100 μM IFNA2 in formulation buffer and a gradient of BA concentrations were used. Samples included 0%, 0.3%, 0.6%, and 0.9% (v/v) BA. HSQC spectra were collected over 8 h. Changes in the cross-peak positions (chemical shifts) were calculated using the nmrDraw package (Frank Delaglio, National Institutes of Health). IFNA2 residue assignments available in the literature[33] were used for this purpose.

Hydrogen Exchange

2D ^{15}N-^{1}H HSQC experiments were run to monitor changes in IFNA2 amide cross peaks as a function of BA concentration using a Varian Inova 900 MHz NMR instrument equipped with a cryoprobe. For these experiments, 200 μM IFNA2 (0.05 M deuterated acetic acid, 0.02% sodium azide, pH 3.5 as measured using a standard hydrogen electrode) was used. A time-zero HSQC of IFNA2 was recorded in aqueous buffer (0.05 M acetic acid, 0.02% sodium azide, pH 3.5) prior to exchange. Buffer exchange was carried out on a Q-Sepharose size-exclusion column (bed volume 4.5 mL), and HSQC spectra were recorded every hour. Changes in peak positions and volumes were calculated using the nmrDraw package.

RESULTS

BA Induces IFNA2 Aggregation

Previous work has demonstrated that BA causes aggregation of pharmaceutical proteins over a course of several days and months when stored at 4°C or at room temperature.[6–10,34–36] Because of these long incubation times, screening the effect of various BA concentrations on protein aggregation is not feasible on a convenient laboratory time scale. Therefore, we accelerated aggregation kinetics by performing isothermal incubation studies at a higher temperature, following the protocols used in earlier studies.[6–10,34–36] Using elevated temperatures to accelerate protein aggregation is becoming a commonly used method for scanning the effect of a large number of solution conditions on protein stability and aggregation.[37–39] In addition, our earlier work on the aggregation of the model protein Cyt *c* showed that the mechanism by which BA and other APs induce protein aggregation is identical at low temperature as well as at high temperature.[18–20] Using size-exclusion chromatography, we show that BA caused IFNA2 monomer loss as a function of the incubation time at 50°C (Fig. 2a). After one day of incubation in the absence of BA, approximately 90% of IFNA2 monomer remained in solution. A similar result was seen in the presence of 0.3% (v/v) BA. However, no monomer was detected after 8 h in the presence of 0.9% (v/v) BA. We then examined the effect of BA concentration on the real-time isothermal kinetics of BA-induced protein aggregation by monitoring the increase in optical density due to the increase in solution turbidity.[28] With the increase of BA concentration, the IFNA2 aggregation kinetics was accelerated (Fig. 2b).

BA Decreases the Temperature at Which IFNA2 Aggregates

An alternative method used in the literature to probe the effects of various solution conditions is to monitor their influence on the temperature at which the protein aggregates during thermal scanning.[6–10,18–20,34–39] For this purpose, we measured the optical density at 450 nm.[29] At this wavelength, the protein and

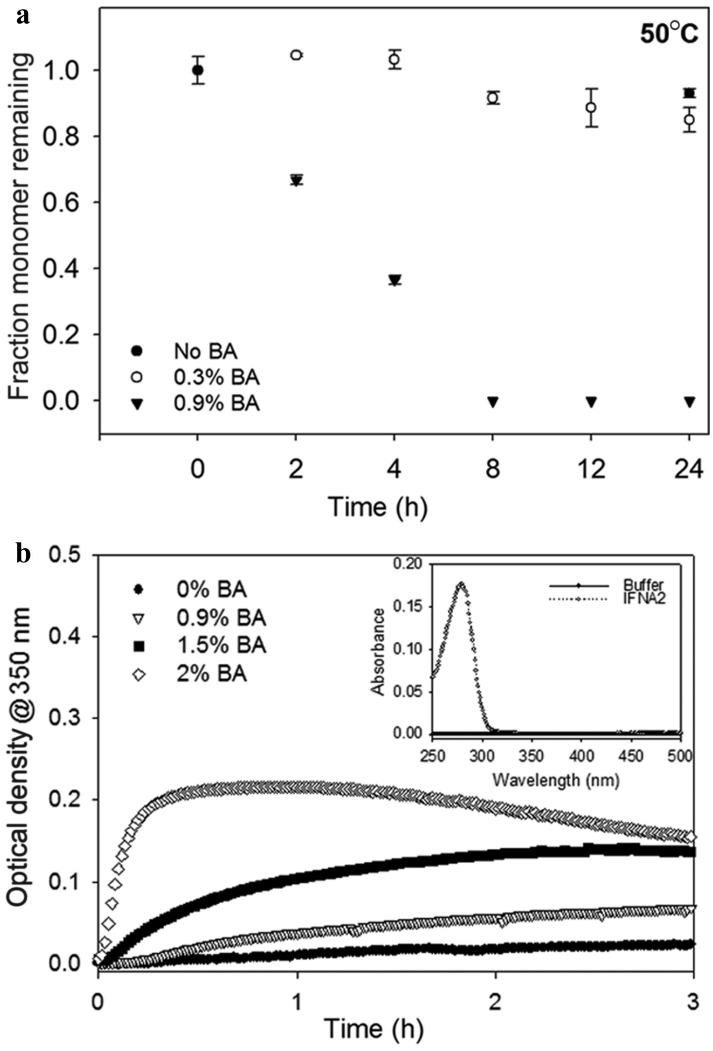

Figure 2. Effects of BA on IFNA2 aggregation under isothermal conditions. (a) Soluble monomer remaining in solution during 24 h of incubation at 50°C in the presence of no BA (closed circles), 0.3% (v/v) BA (open circles), and 0.9% (v/v) BA (closed triangles). Error bars indicate triplicate data. Individual time points are normalized with respect to no BA at 0 h. (b) Aggregation kinetics at 42°C with varying concentrations of BA: 0% (v/v) (closed circles), 0.9% (v/v) (open circles), 1.5% (v/v) (closed triangles), and 2% (v/v) (open triangles). Inset shows absorbance traces for buffer and IFNA2, indicating that neither IFNA2 nor the buffer have absorbance at 350 nm.

the buffer do not absorb (Fig. 2b, inset), and hence the observed changes in the optical density can be attributed solely to protein aggregation. The signal initially increased with increasing temperature and reached a plateau. At higher temperatures, the optical density decreased as protein aggregates began to settle to the bottom of the cuvette. We performed this thermal scanning experiment in the presence of varying concentrations of BA to measure its effect on the T_m^{Agg} of IFNA2 (Fig. 3a). With the addition of BA, IFNA2 melted at lower temperatures, resulting in a decrease of the T_m^{Agg}. In the absence of BA, the T_m^{Agg} was 63.9 ± 0.9°C, whereas the addition of 2% (v/v) BA decreased the T_m^{Agg} to 42.1 ± 0.3°C, indicating that the presence of BA enhanced IFNA2 aggregation.

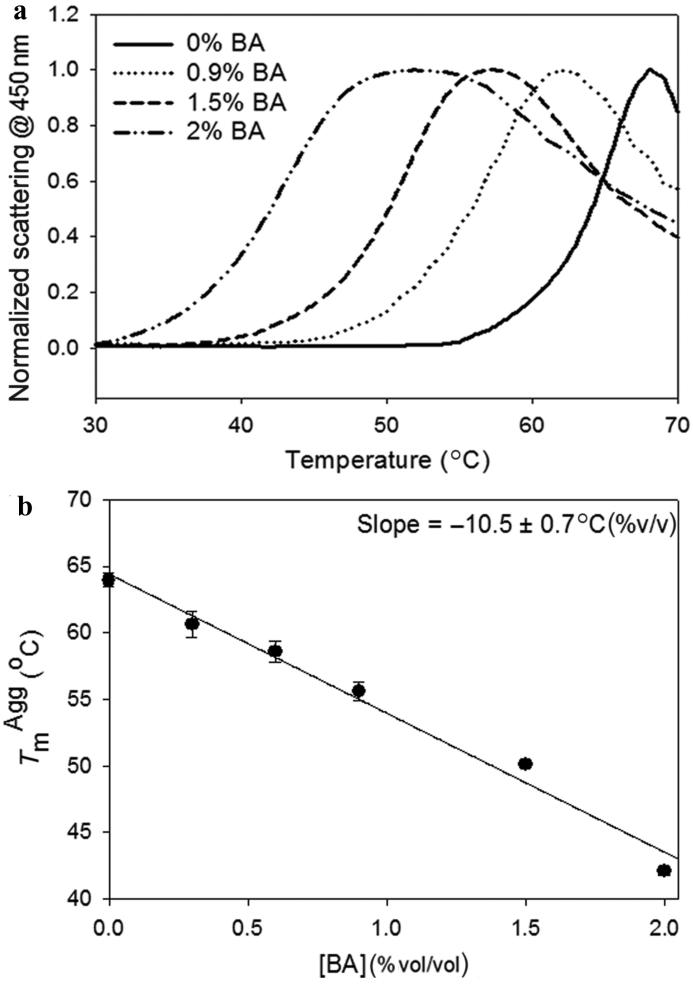

Figure 3. Thermal scanning of IFNA2 in the presence of BA. (a) Variation in the optical density at 450 nm as a function of increasing temperature and varying concentrations of BA. (b) Decrease in T_m^{Agg} as a function of BA concentration.

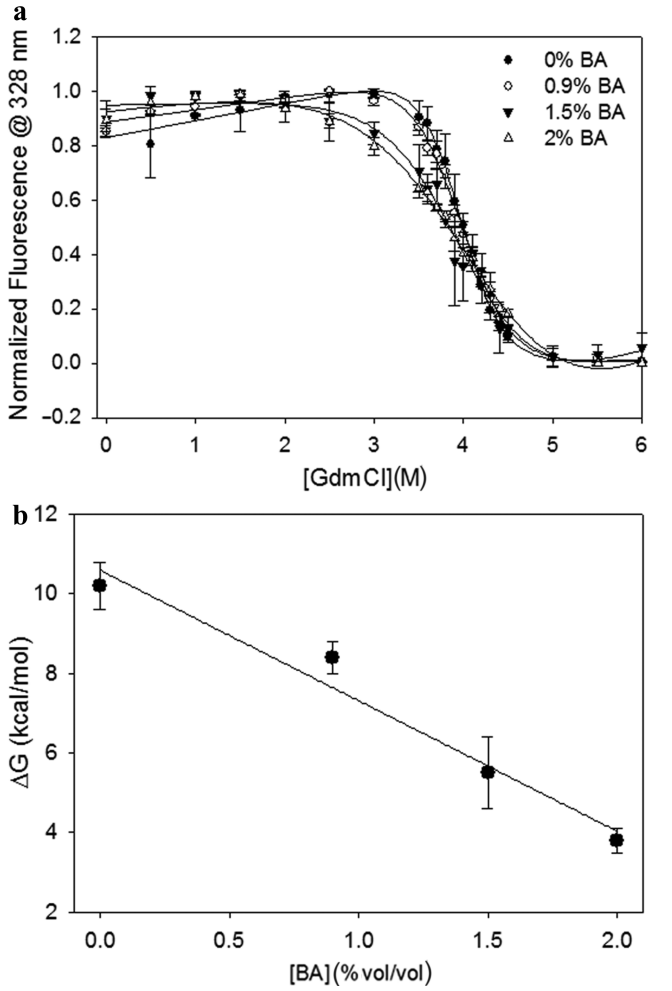

Figure 4. Destabilization of IFNA2 as a function of BA concentration at room temperature. (a) IFNA2 denaturant melts in the presence of varying concentrations of BA: 0% (v/v) (closed circles), 0.9% (v/v) (open circles), 1.5% (v/v) (closed triangles), and 2% (v/v) (open triangles). (b) The free energy of unfolding (ΔG) of IFNA2 as a function of BA concentration.

Aggregation Temperature Decreases Linearly with Increase in BA Concentration

The T_m^{Agg} obtained from thermal scanning experiments was plotted as a function of BA concentration (Fig. 3b). A linear correlation was observed between the increase in BA concentration and the decrease in T_m^{Agg} of IFNA2. This linear correlation is very similar to the commonly observed general protein unfolding behavior where thermodynamic stability (ΔG) or the folding rate (k_f) decreases linearly with the addition of denaturant.[31,32,40] This correlation is significant in that it is a qualitative measure of how effective BA is in inducing aggregation of IFNA2. The effectiveness is reflected in the value of the slope of T_m^{Agg} decrease with increase in BA concentration. The corresponding slope for BA indicates that for every percent increase of BA, the T_m^{Agg} of IFNA2 decreases by 10.5°C (Fig. 3b).

BA Causes Destabilization of IFNA2

In order to monitor the effect of BA on IFNA2 thermodynamic stability, we followed changes in protein intrinsic fluorescence as a function of BA and denaturant concentration (Fig. 4a).

Table 1. Parameters Obtained from Fitting Denaturant Melt Data in Figure 4 to a Two-State Unfolding Model

BA (%, v/v)	ΔG (kcal/mol)	m (kcal/(mol. M [GdmCl]))	C_m (M [GdmCl])
0.0%	10.2 ± 0.6	−2.6 ± 0.2	3.9 ± 0.02
0.9%	8.4 ± 0.4	−2.1 ± 0.1	4.0 ± 0.09
1.5%	5.5 ± 0.9	−1.4 ± 0.2	3.9 ± 0.02
2.0%	3.8 ± 0.3	−0.9 ± 0.1	4.2 ± 0.16

The decrease in m-value with no significant change in C_m implies the presence of an intermediate.

With the addition of increasing concentrations of BA, the calculated ΔG decreased significantly (Fig. 4b). For example, in the absence of BA, the calculated ΔG for IFNA2 was 10.2 ± 0.6 kcal/mol. With the addition of 2% (v/v) BA, the ΔG value dropped to 3.8 ± 0.3 kcal/mol. These denaturant melts indicate that BA causes protein destabilization. Changes in the corresponding m-values were also observed (Table 1). The m-value is a measure of the accessible surface area that is exposed upon protein unfolding.[41] One possible explanation for the decrease

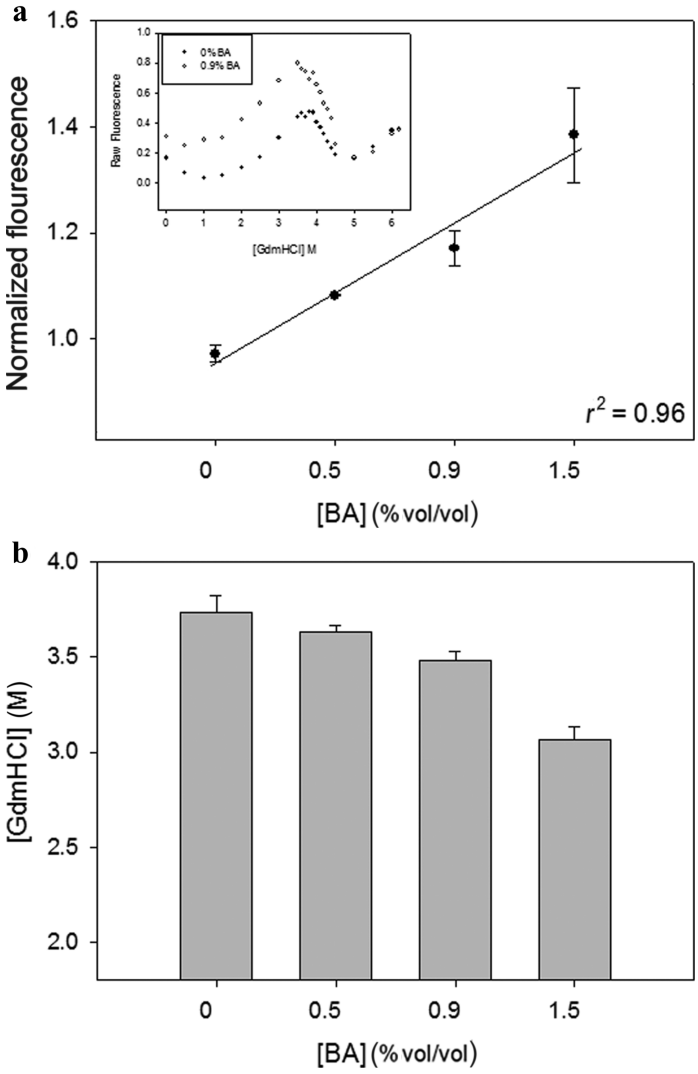

Figure 5. Intermediate detection using ANS as a function of BA concentration in the presence of the denaturant GdmCl at room temperature. (a) Increase in fluorescence emission intensity of ANS as a function of BA concentration, normalized using a rhodamine cuvette. Inset shows representative raw ANS intensity curves as a function of GdmCl concentration at 0% (v/v) BA (closed circles) and 0.9% (v/v) BA (open circles). (b) Comparison of midpoint denaturant concentration at maximum ANS intensity with the addition of BA.

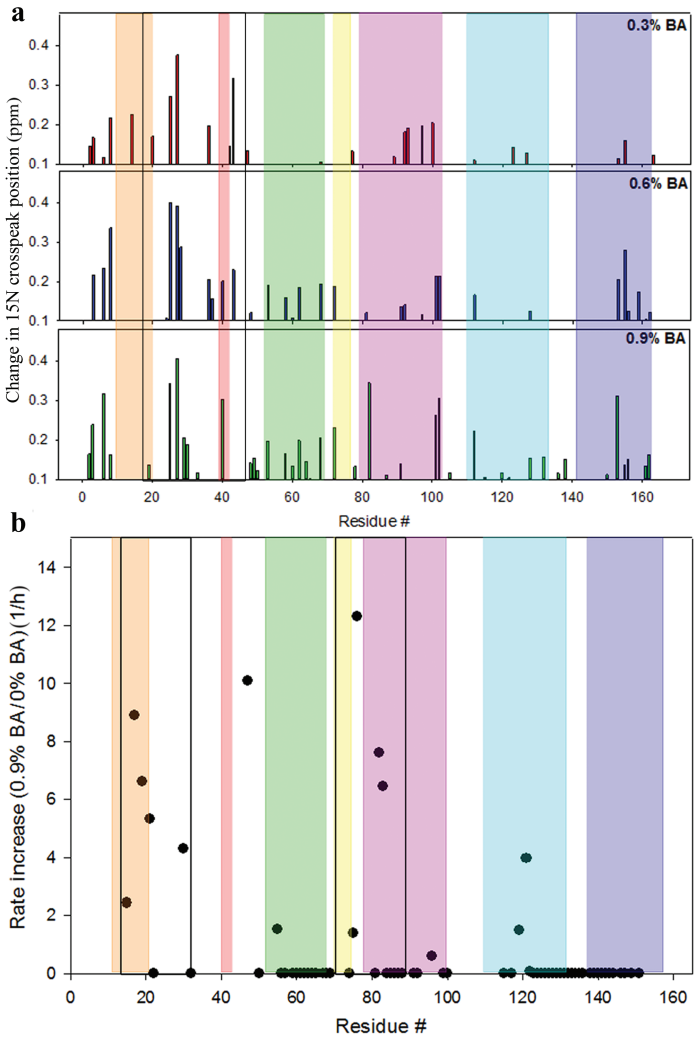

Figure 6. 2D ^{15}N-^{1}H HSQC NMR spectra of IFNA2 in the presence of BA. (a) Chemical shift changes as a function of BA concentration in the ^{15}N dimension. The changes in cross-peak positions represent the absolute changes from 0% (v/v) BA. Top panel: 0.3% (v/v) BA; middle panel: 0.6% (v/v) BA; bottom panel: 0.9% (v/v) BA. The black rectangle shows the region with the highest chemical shift changes when compared with 0% (v/v) BA. (b) HX rates in IFNA2 plotted as a function of residue position. The rate values represent the relative increase of individual amide exchange rates in the presence of 0.9% (v/v) BA when compared with 0% (v/v) BA. Colored bars indicate helices: orange (helix A), red (3_{10} helix), green (helix B), yellow (helix B′), purple (helix C), cyan (helix D), and dark blue (helix E). Black rectangles show maximum HX rate changes when compared with 0% (v/v) BA.

in *m*-value while maintaining the same midpoint (C_m) is the presence of an intermediate.[42]

BA Preferentially Populates an Intermediate

In order to further test the increased population of an intermediate in the presence of BA, we used the hydrophobic fluorescent dye ANS. Increase in ANS fluorescence has been used to detect partially unfolded intermediate states in the presence of GdmCl.[43] The denaturant concentration at which maximum ANS fluorescence was observed was used for comparative purposes. With increasing concentrations of BA, the denaturant concentration at which ANS intensity was highest shifted to lower values, indicating an earlier onset of partial protein unfolding and increased intermediate population (Fig. 5). For example, in the presence of 0% (v/v) BA, maximum ANS fluorescence was observed at 3.7 M GdmCl. In contrast, 1.5% (v/v) BA shifted the denaturant concentration at which ANS fluorescence was maximum to 3.0 M GdmCl.

BA Perturbs IFNA2 Locally

To better understand the specific effects of BA on IFNA2 structure, 2D ^{1}H-^{15}N HSQC NMR spectra were recorded at various BA concentrations. With an increase in BA concentration, numerous ^{1}H-^{15}N cross peaks were perturbed, which were monitored through chemical shift changes. These changes were used to identify the local regions in IFNA2 that were most susceptible to influences by BA (Fig. 6a). For all concentrations of BA,

^{1}H chemical shift changes were less than 0.1 ppm. However, multiple residues demonstrated significant chemical shift alterations (i.e., greater than 0.1 ppm) in the ^{15}N dimension. The most substantial changes were observed in residues within the AB-loop and helix A (Figs. 1 and 6a). For example, between 0% and 0.3% (v/v) BA, the ^{15}N chemical shift of F27 increased by nearly 0.4 ppm. As BA concentration was increased, changes in chemical shifts were observed across the entire protein, indicating that the unfolding propagates to other protein regions.

Hydrogen exchange (HX) experiments in the presence and absence of BA were conducted in order to monitor the effects of BA on structural stabilities around individual amides (Fig. 6b). Nearly all the residues in the AB-loop exchanged within the deadtime of the experiment (2 min), including residue F27, demonstrating that the AB-loop is the most dynamic region of IFNA2. Residues L17, A19, M21, and L30 demonstrated significantly increased exchange rates in the presence of 0.9% (v/v) BA. These residues are located within the C-terminus of helix A and the AB-loop. Additionally, W76, D82, and K83 in helix C showed increased exchange with the addition of BA. In the 3D structure of IFNA2, L17 docks against K83 and has a contact area of 45.3 Å^2 (contact maps were determined using the online server http://ligin.weizmann.ac.il/cma/). Residue M21 and W76 have a similar relationship, with a contact area of 33.4 Å^2 (Fig. 7).

In light of the HX results that show partial protein unfolding, we used computational programs available in the literature to identify the protein regions that may act as "hot-spots" for aggregation.[44–46] Protein aggregation is a multimolecular reaction that is governed by hydrophobic interactions, secondary structural elements, electrostatics, and other physical properties.[44,47,48] Aggregation prediction programs, such as TANGO[44] and AGGRESCAN,[45] take these parameters into account and determine the specific regions that are aggregation prone. The 3D analysis program ZipperDB[46] uses the available

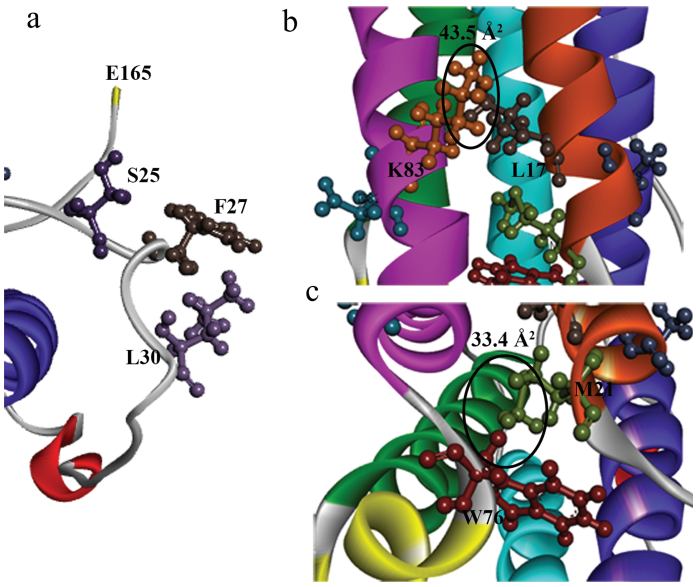

Figure 7. Amino acid contacts within IFNA2 3D structure. (a) Critical residues in the AB-loop are not protected through intraprotein contacts and are highly labile in the native state. (b) Residue L17 in helix A shares a contact area of 43.5 Å^2 with K83 in helix C. (c) Residue M21 in helix A shares a contact area of 33.4 Å^2 with W76 in helix C.

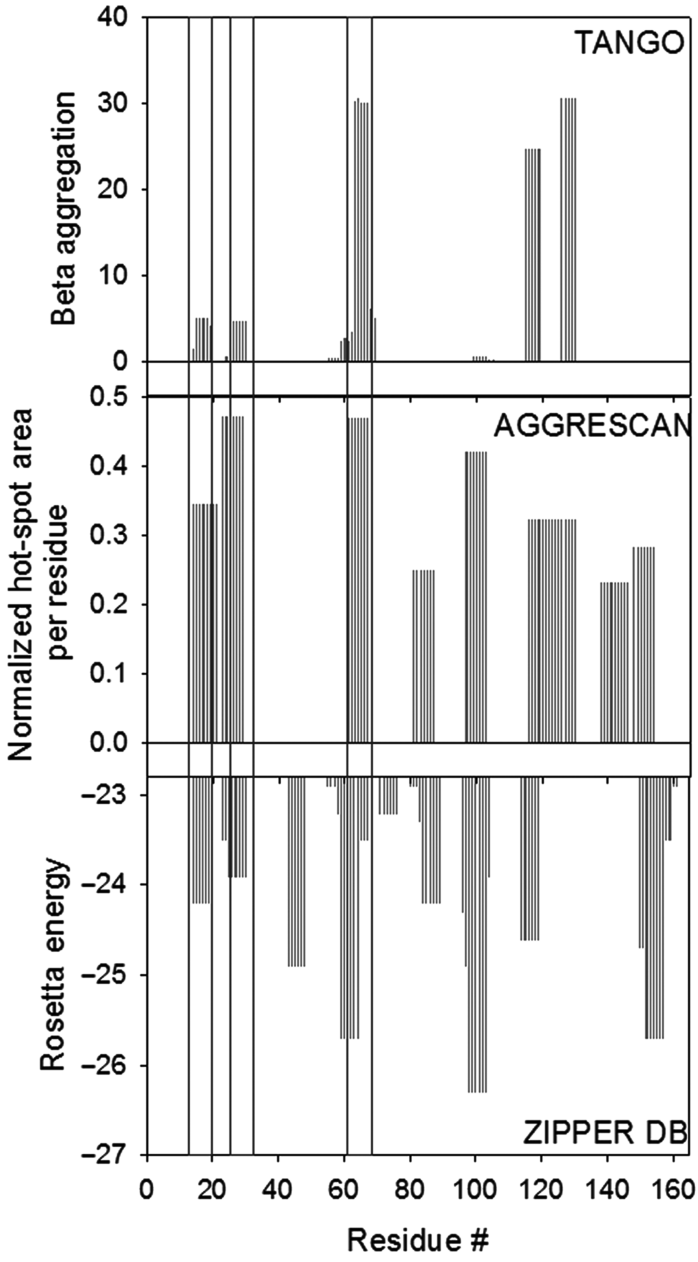

Figure 8. Aggregation propensity predictions for IFNA2 by various computational programs. Black rectangles indicate overlapping regions that were predicted to be aggregation hot-spots by all the three programs.

structure of a protein to determine its propensity for forming cross-β structure, the most common structure found in protein aggregates. These programs were used in conjunction to identify three common aggregation hot-spots in IFNA2 that were predicted by all the programs (Fig. 8). One of these predicted hot-spots is within the highly dynamic AB-loop, which has very little protection in the 3D structure of IFNA2. Another identified hot-spot is located within helix A, a highly ordered α-helical region. BA appears to affect multiple areas of IFNA2 to varying degrees, but imparts significant influence on the AB-loop and within helix A, as evidenced by large changes observed in chemical shifts and HX rates for many amino acids in this region (Fig. 6). The third predicted hot-spot is within helix D,

DOI 10.1002/jps.24105

which did not show significant changes in either the titration experiment or HX, demonstrating the importance of performing experimental studies using high-resolution techniques such as NMR rather than relying upon computational predictions.

DISCUSSION

Multidose formulations require the inclusion of APs to combat the growth of bacteria and other microbes during administration and storage.[3–5] However, recent studies have suggested a link between the presence of APs and protein aggregation.[3–6,9,10,34–36] The ideal method of understanding aggregation mechanisms is to study how various APs induce the aggregation of a pharmaceutical protein of interest using biophysical methods. In our previous work, we used a model protein, Cyt *c*, which has been well characterized in the literature, to monitor preservative-induced protein aggregation mechanisms in response to various stresses.[18–20] We demonstrated that BA, the most commonly used preservative in liquid formulation, caused protein aggregation, and the aggregation was preceded by a local unfolding event rather than global unfolding of the entire protein. This result was significant in that it was the first study to identify the interaction of BA with proteins as mechanistically local in nature, rather than global. Using NMR and other high-resolution techniques provided a clear advantage in structurally identifying the partial unfolding, when compared with other AP-induced aggregation studies performed in the literature.

In the present study, we tested the conclusions obtained from our model system on a pharmaceutically relevant protein IFNA2. IFNA2 is one of 13 interferon-α subtypes found in humans and belongs to the cytokine family of proteins, which plays critical roles in the innate immune response. Interferons are naturally produced as a result of viral or microbial infections and activate a nonspecific, self-perpetuating response by binding to cell surface receptors to initiate a downstream cascade of antiproliferative and antiviral factors.[49–53] As a result, interferon-based pharmaceuticals are used to treat numerous debilitating diseases including various leukemias and hepatitis C.[54]

Interferon α-2a therapeutic formulations have been known to aggregate for nearly two decades.[21–24] Numerous studies have been performed to demonstrate the occurrence of IFNA2 aggregation in therapeutic formulations. For example, in the late 1990s, Hochuli[23] tested IFNA2 formulations for aggregates and determined that the inclusion of human serum albumin (HSA) increased the aggregation propensity of IFNA2. As a result, HSA was removed from the formulation design and replaced with polysorbate 80 as a stabilizer. However, IFNA2 formulations still contain a measurable population of aggregates. In this work, we have shown that BA, the AP used in IFNA2 formulations, also causes protein aggregation, adding a new dimension to IFNA2 aggregation phenomenon under formulation conditions. The 2D-NMR solution structure for IFNA2 has already been solved,[33] which provided a clear advantage in expediting the structural studies to monitor changes on an amino acid level induced by BA.

The influence of BA on IFNA2 stability and aggregation was monitored with numerous biophysical techniques. BA was shown to induce IFNA2 aggregation in a concentration-dependent manner (Figs. 2 & 3). Thermodynamic stability (ΔG) of IFNA2 decreased in the presence of increasing concentrations of BA, with a constant C_m but a changing m-value (Fig. 4). The m-value is related to the differences in the accessible surface areas of the protein's folded and unfolded states. Changes in this value suggest a deviation from two-state behavior, and may indicate the presence of a partially unfolded intermediate.[42] Using the hydrophobic fluorescent dye ANS, we demonstrated that IFNA2 contains such an intermediate that is preferentially populated in the presence of BA (Fig. 5). The identity of this intermediate was determined using high-resolution 2D-NMR and HX techniques, demonstrating that the AB-loop and helix A were specifically influenced by the presence of BA in solution (Fig. 6).

Multiple aggregation propensity programs were utilized to determine potential aggregation "hot-spots" in IFNA2 (Fig. 8). Two of the predicted "hot-spots" were significantly perturbed in the presence of BA (Fig. 6), and these regions share significant surface contacts in the folded protein structure (Fig. 7). It is possible that unfolding of one or both of these regions leads to the formation of the partially unfolded intermediate. BA may be influencing this region by simply disrupting the contacts between these critical residues and initiating a local unfolding event that populates an aggregation-prone species. These data indicate that the AB-loop and the terminus of helix A may play a major role in initiating IFNA2 aggregation.

Another possible interpretation is the disruption of these contacts causes a domain swap, leading to new interhelical connections in a native-like configuration. Significant chemical shift changes were observed in helix A and the AB-loop, indicating that the amino acids in this region move with the addition of BA. A number of other protein examples demonstrate the relationship between domain swapping and the formation of protein aggregates.[55,56] Additionally, Cyt *c* has been shown to assemble into higher order species in the presence of ethanol through the successive swapping of helices from one monomer to another monomer.[57]

Similar to Cyt *c*,[18–20] stabilizing the aggregation "hot-spots" of IFNA2 via specific mutations may reduce BA-induced aggregation. Previous work using alanine scanning demonstrated that a number of residues located in the AB-loop are critical for receptor binding, including F27, L30, and K31.[58–60] Accordingly, introducing a stabilizing mutation at this location could alter protein activity significantly. On the other hand, IFNA2 has been pegylated in recent formulations in order to increase the drug lifetime by protecting the protein from proteolytic degradation, and has been shown to inhibit aggregation.[61,62] Pegylation occurs at six locations in IFNA2 including at K31 in the AB-loop. This positional isomer has very low affinity to the receptor compared with the unmodified IFNA2 (520 and 5 nM, respectively). However, the opposite effects of pegylation on protein stability and activity seem to cancel each other due to increased net protein concentration available for function. It is possible that mutating residues within the AB-loop may confer stability at the cost of potency. Mutating a pharmaceutical protein to minimize aggregation must be performed carefully to ensure that the modified drug product maintains efficacy and safety.

Understanding the specific effects of preservatives on protein systems is critical to the development of safer and more potent protein pharmaceuticals. Our results suggest that the BA influences model proteins and pharmaceutical proteins in a similar manner. In-depth studies on other protein

formulations in the presence of APs are required in order to further test the principles we have demonstrated here for IFNA2 and for Cyt *c*. Probing the specific mechanism of interaction between APs and proteins will be useful in the development of stable pharmaceuticals.

ACKNOWLEDGMENTS

The authors thank John Carpenter, Theodore Randolph, David Bain, and LaToya Jones Braun for many helpful discussions and critical comments. This work was funded by the University of Colorado Skaggs School of Pharmacy and Pharmaceutical Sciences. Regina Bis was partially supported by a NIH Leadership training grant in Pharmaceutical Biotechnology (T32GM008732) and a predoctoral fellowship from the PhRMA Foundation (AWD-120487). Rocky Mountain Regional 900 MHz NMR Facility was funded by the National Institutes of Health instrumentation Grant P41GM068928.

REFERENCES

1. Manning MC, Chou DK, Murphy BM, Payne RW, Katayama DS. 2010. Stability of protein pharmaceuticals: An update. Pharm Res 27:544–575.
2. Trissel LA. 2010. Handbook on injectable drugs. 16th ed. American Society of Health-System Pharmacists, Inc, Bethesda, Maryland.
3. Meyer BK, Ni A, Hu B, Shi L. 2007. Antimicrobial preservative use in parenteral products: Past and present. J Pharm Sci 96:3155–3167.
4. Cleland JL, Powell MF, Shire SJ. 1993. The development of stable protein formulations—A close look at protein aggregation, deamidation and oxidation. Crit Rev Ther Drug Carrier Syst 10:307–377.
5. Akers MJ, Vasudevan V, Stickelmeyer M. 2002. Formulation development of protein dosage forms. In: Nail SL, Akers MJ, editors. Development and manufacture of protein pharmaceuticals. New York: Kluwer Academic/ Plenum Publishers, pp 47–127.
6. Maa YF, Hsu CC. 1996. Aggregation of recombinant human growth hormone induced by phenolic compounds. Int J Pharm 140:155–168.
7. Zhang Y, Roy S, Jones LS, Krishnan S, Kerwin BA, Chang BS, Manning MC, Randolph TW, Carpenter JF. 2004. Mechanism for benzyl alcohol-induced aggregation of recombinant human interleukin-1-receptor antagonist in aqueous solution. J Pharm Sci 93:3076–3089.
8. Roy S, Jung R, Kerwin BA, Randolph TW, Carpenter JF. 2005. Effects of benzyl alcohol on aggregation of recombinant human interleukin-1-receptor antagonist in reconstituted lyophilized formulations. J Pharm Sci 94:382–396.
9. Tobler SA, Holmes BW, Cromwell MEM, Fernandez EJ. 2004. Benzyl alcohol-induced destabilization of interferon-γ. J Pharm Sci 93:1605–1617.
10. Gupta S, Kaisheva E. 2003. Development of a multidose formulation for a humanized monoclonal antibody using experimental design techniques. AAPS Pharm Sci 5:1–9.
11. Rosenberg AS. 2006. Effects of protein aggregation: An immunologic perspective. AAPS J 8:E501–E507.
12. Bucciantini M, Giannoni E, Chiti F, Baroni F, Formingli L, Zurdo J, Taddei N, Ramponi G, Dobson CM, Stefani M. 2002. Inherent toxicity of aggregates implies a common mechanism for protein misfolding diseases. Nature 416:507–511.
13. Fradkin AH, Carpenter JF, Randolph TW. 2009. Immunogenicity of aggregates of recombinant human growth hormone in mouse models. J Pharm Sci 98:3247–3264.
14. Ratner RE, Phillips TM, Steiner M. 1990. Persistent cutaneous insulin allergy resulting from high molecular weight insulin aggregates. Diabetes 39:728–733.
15. Sauerborn M, Brinks V, Jiskoot W, Schellekens H. 2010. Immunological mechanism underlying the immune response to recombinant human protein therapeutics. Trends Pharmacol Sci 31:53–59.
16. Vazquez-Rey M, Lang DA. 2011. Aggregates in monoclonal antibody manufacturing processes. Biotechnol Bioeng 108:1494–1508.
17. Hermeling S, Schellekens H, Maas C, Gebbink MF, Crommelin DJ, Jiskoot W. 2006. Antibody response to aggregated human interferon alpha2b in wild-type and transgenic immune tolerant mice depends on type and level of aggregation. J Pharm Sci 95:1084–1096.
18. Hutchings RL, Singh SM, Cabello-Villegas J, Mallela KMG. 2013. Effect of antimicrobial preservatives on partial protein unfolding and aggregation. J Pharm Sci 102:365–376.
19. Singh SM, Hutchings RL, Mallela KMG. 2011. Mechanisms of m-cresol-induced protein aggregation studied using a model protein cytochrome *c*. J Pharm Sci 100:1679–1689.
20. Singh SM, Cabello-Villegas J, Hutchings RL, Mallela KMG. 2010. Role of partial protein unfolding in alcohol-induced protein aggregation. Proteins 78:2625–2637.
21. Braun A, Alsenz J. 1997. Development and use of enzyme linked immunosorbent assays (ELISA) for the detection of protein aggregates in interferon-alpha (IFN-α) formulations. Pharm Res 14:1392–1400.
22. Braun A, Kwee L, Labow MA, Alsenz L. 1997. Protein aggregates seem to play a key role among the parameters influencing the antigenicity of interferon alpha (IFN-α) in normal and transgenic mice. Pharm Res 14:1472–1478.
23. Hochuli E. 1997. Interferon immunogenicity: Technical evaluation of interferon-α2a. J Interferon Cytokine Res 17:S15–S21.
24. Ryff J. 1997. Clinical investigation of the immunogenicity of interferon-α2a. J Interferon Cytokine Res 17:S29–S33.
25. Mossessova E, Lima CD. 2000. Ulp1-SUMO crystal structure and genetic analysis reveal conserved interactions and a regulatory element essential for cell growth in yeast. Mol Cell 5:865–876.
26. Lima CD, Mossessova E. 2005. Rapidly cleavable sumo fusion protein expression system for difficult to express proteins. Patent #US7910364 B2.
27. Bis RL, Stauffer TM, Singh SM, Lavoie TB, Mallela KM. 2014. High yield soluble bacterial expression and streamlined purification of recombinant human interferon α-2a. Protein Expr Purif 99:138–146.
28. Eckhardt B, Oeswein J, Yeung D, Milby T, Bewley T. 1994. A turbidimetric method to determine visual appearance of protein solutions. J Pharm Sci Tech 48:64–70.
29. Charman S, Mason K, Charman W. 1993. Techniques for assessing the effects of pharmaceutical excipients on the aggregation of porcine growth hormone. Pharm Res 10:954–962.
30. Pace CN. 1986. Determination and analysis of urea and guanidine hydrochloride denaturation curves. Methods Enzymol 131:266–280.
31. Santoro MM, Bolen DW. 1992. A test of the linear extrapolation of unfolding free energy changes over an extended denaturant concentration range. Biochemistry 31:4901–4907.
32. Santoro MM, Bolen DW. 1988. Unfolding free energy changes determined by the linear extrapolation method. 1. Unfolding of phenylmethanesulfonyl alpha-chymotrypsin using different denaturants. Biochemistry 27:8063–8068.
33. Klaus W, Gsell B, Labhardt A, Wipf B, Senn H. 1997. The three-dimensional high resolution structure of human interferon α-2a determined by heteronuclear NMR spectroscopy in solution. J Mol Biol 274:661–675.
34. Remmele Jr. RL, Nightlinger NS, Srinivasan S, Gombotz WR. 1998. Interleukin-1 receptor (IL-1R) liquid formulation development using differential scanning calorimetry. Pharm Res 15:200–208.
35. Roy S, Katayama D, Dong A, Kerwin BA, Randolph TW, Carpenter JF. 2006. Temperature dependence of benzyl alcohol- and 8-anilinonaphthalene-1-sulfonate-induced aggregation of recombinant human interleukin-1 receptor antagonist. Biochemistry 45:3898–3911.
36. Thirumangalathu R, Krishnan S, Brems DN, Randolph TW, Carpenter JF. 2006. Effects of pH, temperature, and sucrose on benzyl alcohol-induced aggregation of recombinant human granulocyte colony stimulating factor. J Pharm Sci 95:1480–1497.

37. Nashine VC, Kroetsch AM, Sahin E, Zhou R, Adams ML. 2013. Orthogonal high-throughput thermal scanning method for rank ordering protein formulations. AAPS PharmSciTech 14:1360–1366.
38. Chaudhuri R, Cheng Y, Middaugh CR, Volkin DB. 2014. High-throughput biophysical analysis of protein therapeutics to examine interrelationships between aggregate formation and conformational stability. AAPS J 16:48–64.
39. Brummitt RK, Nesta DP, Roberts CJ. 2011. Predicting accelerated aggregation rates for monoclonal antibody formulations, and challenges for low-temperature predictions. J Pharm Sci 100:4234–4243.
40. Gianni S, Ivarsson Y, Jemth P, Brunori M, Travaglini-Allocatelli C. 2007. Identification and characterization of protein folding intermediates. Biophys Chem 128:105–113.
41. Myers JK, Pace CN, Scholtz JM. 1995. Denaturant m values and heat capacity changes: Relation to changes in accessible surface areas of protein unfolding. Protein Sci 4:2138–2148.
42. Scholtz JM, Grimsley GR, Pace CN. 2009. Solvent denaturation of proteins and interpretations of the m value. Methods Enzymol 466:549–565.
43. Vazquez-Contreras E, Zubillaga R, Mendoza-Hernandez G, Costas M, Fernadez-Velasco D. 2000. Equilibrium unfold of yeast triosephosphate isomerase: A monomeric intermediate in guanidine-HCl and two-state behavior in urea. Prot Pept Lett 7:57–64.
44. Fernandez-Escamilla A-M, Rousseau F, Schymkowitz J, Serrano L. 2004. Prediction of sequence-dependent and mutational effects on the aggregation of peptides and proteins. Nat Biotech 22:1302–1306.
45. Conchilli-Solé O, de Groot NS, Avilés FX, Vendrell J, Daura X, Ventura S. 2007. AGGRESCAN: A server for the prediction and evaluation of "hot-spots" of aggregation in polypeptides. BMC Bioinformatics 8:65.
46. Goldschmidt L, Teng PK, Riek R, Eisenberg D. 2010. Identifying the amylome, proteins capable of forming amyloid-like fibrils. Proc Natl Acad Sci USA 107:3487–3492.
47. Chiti F, Stefani M, Taddei N, Ramponi G, Dobson CM. 2003. Rationalization of the effects of mutations on peptide and protein aggregation rates. Nature 424:805–808.
48. de Groot NS, Pallarés I, Avelés FX, Vendrell J, Ventura S. 2005. Prediction of "hot spots" of aggregation in disease-linked polypeptides. BMC Struct Biol 5:18.
49. Fensterl V, Sen GC. 2009. Interferons and viral infections. BioFactors 35:14–20.
50. Jonasch E, Haluska F. 2001. Interferons in oncological practice: Review of interferon biology, clinical applications, and toxicity. Oncologist 6:34–55.
51. Kaser A, TILG H. 2000. Interferon-α in inflammation and immunity. Cell Mol Biol 47:609–617.
52. Malmagaard L. 2004. Induction and regulation of IFNs during viral infections. J Interferon Cytokine Res 24:439–454.
53. Theofilopoulos AN, Baccala R, Beutler B, Kono DH. 2005. Type I interferons (alpha/beta) in immunity and autoimmunity. Annu Rev Immunol 23:307–336.
54. Kirkwood J. 2002. Cancer immunotherapy: The interferon-alpha experience. Semin Oncol 29:18–26.
55. Carey J, Lindman S, Bauer M, Linse S. 2007. Protein reconstitution and three-dimensional domain swapping: Benefits and constraints of covalency. Protein Sci 16:2317–2333.
56. Liu Y, Eisenberg D. 2002. 3D domain swapping: As domains continue to swap. Protein Sci 11:1285–1299.
57. Hirota S, Hattori Y, Nagao S, Taketa M, Komori H, Kamikubo H, Wang Z, Takahashi I, Negi S, Sugiura Y, Kataoka M, Higuchi Y. 2010. Cytochrome *c* polymerization by successive domain swapping at the C-terminal helix. Proc Natl Acad Sci USA 107:12854–12859.
58. Piehler J, Schreiber G. 1999. Biophysical analysis of the interaction of human IFNAR2 expressed in E. coli with IFNα2. J Mol Biol 289:57–67.
59. Piehler J, Roisman LC, Schreiber G. 2000. New structural and functrional aspects of the type I interferon-receptor interaction revealed by comprehensive mutational analysis of the binding interface. J Biol Chem 275:40425–40433.
60. Piehler J, Schreiber G. 1999. Mutational and structural analysis of the binding interface between type I interferons and their receptor IFNAR2. J Mol Biol 294:233–237.
61. Dhalluin C, Ross A, Leuthold LA, Foser S, Gsell B, Müller F, Senn H. 2005. Structural and biophysical characterization of the 40 KDa PEG-interferon-α2a and its individual positional isomers. Bioconjugate Chem 16:504–517.
62. Dhalluin C, Ross A, Huber W, Gerber P, Brugger D, Gsell B, Senn H. 2005. Structural, kinetic, and thermodynamic analysis of the binding of the 40 KDa PEG-interferon-α2a and its individual positional isomers to the extracellular domain of the receptor IFNAR2. Bioconjuge Chem 16:518–527.